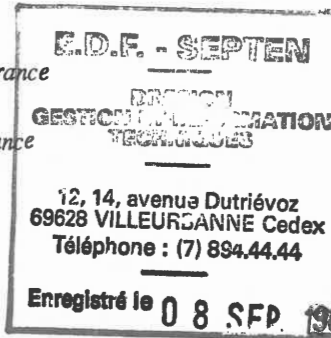


# Fatigue analysis methods of crack like defects

## I. Strain range evaluation

D.Moulin & B.Autrusson  
CEA-CEN Saclay, IRDI-DEMT, Gif-sur-Yvette, France

B.Barrachin  
CEA-CEN Fontenay-aux-Roses, IPSN-DAS, France



### 1 INTRODUCTION

Structural components of nuclear reactors may contain fabrication defects that can propagate under cyclic loading resulting from operating conditions. Such designed defects are, for example, partially penetrated weldments between two components parts. These defects present frequently very sharp extremities that may lead to consider them like cracks for analysis. In such situations fatigue analysis methods for discontinuities as proposed in construction codes like ASME III (1), Code Case N47 (2), RCC-M (3) or RCC-MR (4) are not directly applicable. Special developments are needed. Important work was performed in France in order to derive practical methods to predict fatigue initiation in crack-like defects. Roche in (5) describes some developments accomplished and presents the principles of rules based on strain evaluation at a constant material characteristic distance  $d$  from the notch tip and on the use of a design fatigue initiation curve. This study presented here was performed under financial support of the C.E.A. Safety Authorities-IPSN.

### 2 DESCRIPTION OF PROBLEM

A complementary study presented in (6) shows a practically satisfactory correlation between, simple elastic calculation and prediction of initiation with a design fatigue curve on one hand, with a large compilation of experimental results on the other hand. In this paper an attempt is made to evaluate local strain for this prediction by the use of some elastoplastic analysis methods. These applications concerned a mechanical configuration for which an ad'hoc experimental investigation was performed for comparison.

### 3 DESCRIPTION OF THE EXPERIMENTS

#### 3.1 Experimental device

The experimental investigation concerned 6 rectangular long cantilever beams (see figure 1). The specimen is clamped at one extremity close

to the machined vertical crack. The other extremity is moved cyclically by a conventional testing machine.

The geometrical dimensions are given in figure 1 and in table 1. The cracks are machined so that the notch radius is less than 0.1 mm. The cracks of specimens 2, 3, 4, 5 and 6 are mill-machined. The notch of specimen n°1 is obtained by electro-erosion.

The displacement is imposed to the specimen via a clip-gage transducer clamped at a certain distance of notch section (see figure 1). The strain range  $\Delta\epsilon_2$  in this location is imposed constant during the test until an initiation signal occurs. The  $\epsilon_2$  signal is purely reversed (mean value is zero).

During the test the following parameters are also recorded: the strength P, the deformation  $\epsilon_1$  on the outer skin at opposite side from the crack, the mouth opening displacement  $\delta$ , strain and electric potential drop near the end of the notch (see figure 1).

The specimen are made of a 304 L austenitic steel. The uniaxial cyclic material curve of the sheet from which specimens are extracted is determined. It is characterized by the equation:

$$\frac{\Delta\epsilon}{2} = K \left( \frac{\Delta\sigma}{2} \right)^N \quad \text{where } K = 2177 \text{ and } N = 0.379$$

Table 1. Experimental and calculated data. Plane stresses

Specimen	1	2	3	4	5	6
Initial crack (mm)	49.6	49.8	49.5	40.0	30.1	20.1
$\Delta\epsilon_2 \cdot 10^{-4}$	2.61	5.60	1.04	5.04	3.56	6.80
$\Delta\epsilon_1 \cdot 10^{-4}$	5.60	12.1	2.22	9.62	5.60	9.36
$\frac{\Delta P}{2}$ kN	2.68	5.60	0.98	5.36	3.70	7.20
$\Delta\delta$ (mm)	0.125	0.255	0.051	0.172	0.084	0.100
$\Delta\sigma_{xx}$ (MPa)	1661	3309	662	-	-	-
$\Delta K_I$ (MPa/m)	27.9	60.2	11.1	45.7	26.9	41.3
$\Delta\sigma_{xx}^*$ (MPa)	1673	3603	666	2735	1610	2473
$\overline{\Delta\epsilon}^*$ ( % )	1.43	4.37	0.38	2.93	1.36	2.53
$\overline{\Delta\epsilon}^{**}$ ( % )	2.5	-	0.64	-	-	-
$\overline{\Delta\epsilon}$ ( % )	1.8	-	0.3	-	-	-

\* value non calculated.

### 3.2 Detection of initiation

The electric potential drop measurement is the most rapid and sensible way to determine initiation of crack. A linear correlation for all specimens (except n°3) was found between potential drop recording and mean fronts measurements performed after heat tinting of fronts inside a furnace and fracture of specimens. This calibration straight line is used to define, on graphical potential drop versus time recordings, initiation for 0.1 mm ; 0.5 and 1 mm propagated cracks. This calibration correlates also well with measurements of surface crack propagation revealed by rupture of gauge wires placed near notch end in specimen n°2.

For the number of cycles performed all the other recorded signals give no indication of possible crack initiation: the recorded values do not significantly evolve neither in range nor in amplitude from the values obtained at the first cycle.

For specimen n°1 initiation is only determined from rupture of surface gauge wires.

The various experimental initiation cycles numbers are used in figure 4.

## 4 CALCULATION METHODS

### 4.1 Elastoplastic finite element method

A simplified cyclic method proposed by Dowling (7) is performed. It consists of finite element calculations with refined meshes (see figure 2) modelizing the configuration geometry. The increase of displacement is monotonic. The material plastic behaviour is characterized by usual flow rules and isotropic hardening applied to the cyclic curve. The shell element code INCA, developed in CEA, is used with plane stresses hypothesis. Only one crack depth ( $a = 50$  mm) is considered.

These calculations draw elastic and elastoplastic results presented in table 1. Stress and strain values are taken at the distance  $d = 0.05$  mm from crack tip.  $\Delta \bar{\epsilon}$  is the equivalent strain range calculated with Von Mises criterion.  $\Delta \sigma_{xx}$  is the elastic stress component.

### 4.2 Handbook approach

It is possible to calculate the same elastic global parameters as determined by F.E. calculation with some simple elastic formulae. From imposed deformation  $\Delta \epsilon_2$  elastic equations give the imposed bending moment  $\Delta M$  in the crack section. Using the shape factor of a cracked beam submitted to uniform bending, as proposed in an handbook like (13), the value  $\Delta K_I$  can be evaluated (see table 1).

### 4.3 Creager approximation (8)

This method already discussed in (9) and widely used in (6) permits to calculate elastic strain distribution in the neighbourhood of the crack tip influenced by notch radius from  $K_I$  value. The calculated values  $\Delta \sigma_{xx}^*$  are presented in table 1.

#### 4.4 H.R.R. method

Here an attempt is made to use results of H.R.R. calculations (10) and (11) to evaluate elastoplastic strain in the vicinity of crack tip from calculated J value and material characteristics:

$$\epsilon = \left( \frac{J}{rK \ln} \right)^{\frac{1}{N+1}}$$

where : -  $\ln$  is a contour integral. Here the value is linearly extrapolated from values calculated in (10) in plane stresses.  
-  $r = 0.05$  mm.  
-  $K$  and  $N$  are material constants of the cyclic curve.

The value of strain calculated by the upper formula for J value is compared to equivalent strain range and is noted  $\overline{\Delta\epsilon}^{**}$ . See table 1.

#### 4.5 Neuber correction (12)

This method presented in (5) intends to evaluate elastoplastic strain range from elastic strain range calculations and the use of cyclic material stress-strain curve. The resulting values  $\overline{\Delta\epsilon}^*$  are presented in table 1.

#### 4.6 Comparisons between calculation methods

Concerning elastic results some interesting features are:

- The stress values are larger when notch radius is 0.1 mm compared to  $r = 0$ .
- The evaluation of  $K_{II}$  by simplified handbook method is comparable to the value obtained by F.E. method. The  $K_{III}$  value is low.
- The elastic stress calculated by Creager formula agrees well with elastic F.E. results.

Concerning elastoplastic methods:

- The strain value  $\overline{\Delta\epsilon}$  is not influenced by notch radius.
- The strain values estimations are more and more large according to the following elastoplastic methods: Neuber, elastoplastic F.E. method, "simplified H.R.R." method. See the comparison between the 3 methods in figure 3.

### 5 COMPARISON BETWEEN CALCULATION AND EXPERIMENTS

The comparison, following the principles of construction codes, is possible by using best fit curve, rehaussed best fit curve ( $\times 1.5$  on strain) as proposed in RCC-MR or design fatigue curve of the relevant steel.

The corresponding curves are presented in figure 4.

The representative points are to be compared to them. The points abscissa represents the different experimental numbers of cycles necessary to reach some amount of propagation for each specimen. The point ordinates are here evaluated according to the Creager-Neuber method applied with plane strains conditions. The representative points seem to follow an experimental mean curve somewhat steeper than

the 3 fatigue curves. It goes through the 3 fatigue curves when number of cycles is increased. Largest strain ranges (where plasticity is more important) could be overpredicted. The same comparison is achieved if the various experimental results presented in the following paper (6) are treated in the same manner (see figure 5).

If figures 4 and 5 are now examined in connexion with figure 3 it could be concluded that plasticity corrections obtained from F.E. calculation and H.R.R. method still increase this overprediction for large strains.

## 6 CONCLUSIONS

Elastoplastic calculation methods permit to evaluate more correctly than elastic ones the real strain range at 0.05 mm far from notch tip. When compared to the experimental results by the use of design fatigue curves to predict number of cycles to initiation correlation is not obviously better than elastic methods presented in (6) for practical applications.

For a more precise evaluation of fatigue initiation by elastoplastic methods, some developments seems to be necessary. These could interest the adjustment of the characteristic distance  $d$ .

## REFERENCES

- (1) ASME "Pressure Vessels and Boiler Code. Section III. Nuclear Components". Am. Soc. of Mech. Eng. New York 1983.
- (2) ASME "Code Case N4721 (1592-21) classe 1 Components at elevated temperature". Am. Soc. of Mech. Eng. New York 1985.
- (3) RCC-M. Règles de conception et de construction de matériels mécaniques d'îlots nucléaires REP-AFCEN.
- (4) RCC-MR. Règles de conception et de construction des matériels mécaniques des îlots nucléaires RNR-AFCEN (Edition AFCEN 1983) 1<sup>ère</sup> édition 1985 en vente à l'AFNOR.
- (5) Roche, R., Amorçage des fissures de fatigue dans les singularités géométriques. Note CEA 2408, Juillet 1984.
- (6) Atrusson, B., Moulin, D., Barrachin, B. Fatigue analysis methods of crack-like defects. II. Applications and validations. Paper G.F 7/4. 9<sup>th</sup> SMIRT, Lauzanne, Suisse (1987).
- (7) Dowling, W.E., Wilson, W.K., "Analysis of Notch Strain for Cyclic Loading" L 13/4 - 5 SMIRT.
- (8) Creager, M., (1966) "The elastic stress fold near the Tip of a blunt crack". Thesis Lehigh University.
- (9) Descatha, Y., Devaux, J.C., Bernard J.L. and Pellissier Tanon. "A criteria for analysing fatigue crack. Initiation in geometrical singularities" C 34/80 - 4<sup>th</sup> ICPVT Londres.
- (10) Hutchinson, J.W., "Singular behaviour at the end of a tensile crack in a hardening material". J. Mech. Phys. Solids, pp. 13-31, Vol. 16, 1968.
- (11) Rice, J.R., Rosengren, G.F., "Plane strain deformation near a crack tip in a power hardening material". J. Mech. Phys. Solids, pp. 1-17, Vol. 16, 1968.
- (12) Neuber, H., "Theory of stress concentration for shear strained Prismatic Bodies with Arbitrary New Linear Stresse Strain Law". Trans. A.S.M.E., J. Appl. Mech. Dec., 1961, pp. 544-550.
- (13) Compendium of Stress Intensity Factors. Rooke et al., Hillingdon Press.

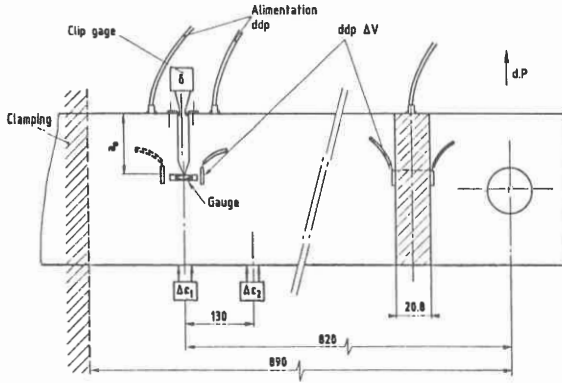


Fig. 1 - Experimental configuration

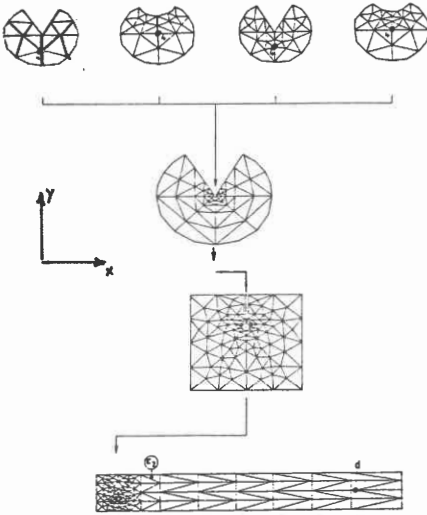


Fig. 2 - Mesh modelizations for FE calculation

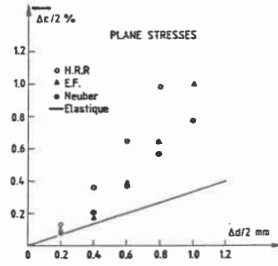


Fig. 3 - Comparison between elastoplastic calculation methods

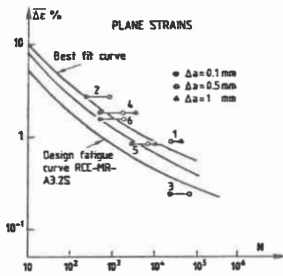


Fig. 4 - Comparison between calculated and experimental results

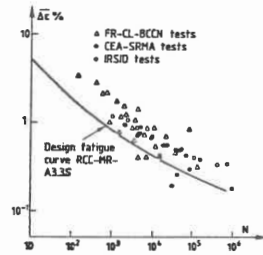


Fig. 5 - Comparison between calculation and experimental results. Plane strains. From [6]